Holocene hydroclimate in the Southeastern United States during abrupt climate events: evidence from new speleothem isotopic records from Alabama

Martín Medina-Elizalde [1*], Stefan Perritano[2], Matthew DeCesare[2], Josué Polanco-Martinez[3], Gabriela Serrato-Marks[4], David McGee[4], Fernanda Lases-Hernandez[5].

1. Department of Geosciences, University of Massachusetts, Amherst.
2. Department of Geosciences, Auburn University, Alabama.
3. DeustoTech-Deusto Institute of Technology, Faculty of Engineering, University of Deusto, Bilbao, Spain.
4. Department of Earth, Atmospheric and Planetary Sciences, Massachusetts Institute of Technology
5. Department of Chemistry (Facultad de Química), National Autonomous University of Mexico (UNAM), Sisal, Yucatán, Mexico.

*Corresponding author: Martín Medina-Elizalde, Email: mmedinaeliza@umass.edu

Abstract

We present new high-resolution absolute-dated stalagmite $\delta^{18}O$ and $\delta^{13}C$ records from Alabama, southeastern United States (SE US), spanning the last 12 thousand years (ka). A local relationship between annual rainfall amount and its amount-weighed $\delta^{18}O$ composition exists on interannual timescales, driven mostly by an amount effect during summer and spring seasons, and by an isotopically depleted composition of fall and winter precipitation. Based on a novel interpretation of modern rainfall isotopic data, stalagmite $\delta^{18}O$ variability is interpreted to reflect the relative contribution of summer and spring precipitation combined relative to combined fall and winter precipitation. Precipitation amount in the SE US increases during the Younger Dryas, the 8.2 ka and Little Ice Age abrupt cooling events. High precipitation during these events reflects enhancement of spring and summer precipitation while the contribution of fall and winter rainfall remained unchanged or decreased slightly. Results from this study support model simulation results that suggest increased precipitation in the SE US during Atlantic Meridional Overturning Circulation (AMOC) slowdown/shutdown (LeGrande et al., 2006; Renssen et al., 2002; Vellinga and Wood, 2002). In association with Northern Hemisphere mid-latitude cooling

from the Early to mid-Holocene, annual precipitation in the SE US decreases, a pattern distinctive from that observed during abrupt cooling events related to AMOC shifts. Long-term hydroclimate change in the SE US is likely sensitive to summer insolation reduction as inferred for other tropical and subtropical regions. This study has implications for our understanding of the sensitivity of subtropical hydroclimate to factors both internal and external to the climate system in a warmer climate.

1. Introduction

The evolution of human societies and ecosystems are intimately related to the degree of climate stability over time at a regional scale (IPBES, 2019; Ipcc, 2014). The Intergovernmental Platform on Biodiversity and Ecosystem Services (IPBES) estimates that within the next three decades 1 million species are threatened with extinction, and it highlights temperature and hydroclimate change as chief driving factors (IPBES, 2019). Large uncertainty remains, however, regarding our understanding of past hydroclimate variability and its underlying drivers, and therefore also, in our capacity to predict the future. Considerable disagreement among state-of-the-art climate model predictions of precipitation for the end of this century underlines the need to better understand the drivers of hydroclimate variability to help improve the climate forecast (Anandhi and Bentley, 2018).

A potential driver of abrupt hydroclimate change relates to climate reorganizations associated with slowdown or complete shutdown of the Atlantic Meridional Overturning Circulation (AMOC). This circulation system is thought to be a key tipping point of the Earth's climate system and seems to already be responding to increasing anthropogenic climate forcings (Collins et al., 2019). The potential impacts of AMOC shifts on Northern Hemisphere hydroclimate remain unclear, however. The historical hydroclimate record remains too short and

55 fragmented to help validate long-term climate model simulations. Thus, model studies rely on
56 the few existing paleoclimate records to assess their performance simulating climate change
57 triggered by abrupt ocean circulation changes (Dahl et al., 2005; Otto-Bliesner and Brady, 2010;
58 Vellinga and Wood, 2002).

59 Hydroclimate variability in the Southeastern United States (SE US) over the Holocene
60 remains poorly understood and model predictions for the end of this century are highly variable,
61 ranging from regional changes of -30 to +35% (Anandhi and Bentley, 2018). The possibility that
62 SE US hydroclimate could respond to abrupt climate change resulting from AMOC shifts exists
63 but remains to be examined with empirical observations.

64 The YD (12.8-11.8 ka) (Rasmussen et al., 2006), the 8.2 ka (Thomas et al., 2007) and the
65 Little Ice Age (LIA, C.E. 1400-1900) (Matthes, 1939) cooling events are hypothesized to be in
66 association with AMOC slowdown/shutdown (Broecker et al., 1989), and they provide a testbed
67 to examine subtropical hydroclimate responses to ocean thermohaline circulation shifts.
68 Paleoclimate and model results support the hypothesis that thermohaline circulation changes
69 triggered the YD and 8.2 ka cooling events (Bard et al., 2000; Lea et al., 2003; LeGrande et al.,
70 2006; Peterson and Haug, 2006; Renssen et al., 2002), and were associated with the LIA (Lund
71 et al., 2006). The extent to which these climate oscillations propagated beyond the North Atlantic
72 high-latitudes and affected subtropical hydroclimate, particularly within the SE US, remains
73 poorly known.

74 There are currently very few paleoclimate records from the SE US that cover the critical time
75 intervals during which ocean thermohaline circulation shifts have been recorded. Available
76 paleoenvironmental records for this region (Goman and Leigh, 2004; Grimm et al., 1993)
77 suggest a pattern of Holocene hydroclimate that does not seem to agree with observations from

78 the North Atlantic over these critical intervals (Grimm et al., 2006). Furthermore, climate model-
79 hosing experiments produce hydroclimate results for the North Atlantic region that are model
80 dependent and strongly contingent upon the duration, magnitude and location of freshwater
81 forcing (Collins et al., 2019; Otto-Bliesner and Brady, 2010).

82 Stalagmite $\delta^{18}O$ records from the North Atlantic offer a unique opportunity to reconstruct the
83 long-term history of precipitation variability from interannual to millennial timescales in low and
84 mid-latitudes (Aharon and Dhungana, 2017; Medina-Elizalde et al., 2017). Currently, there are
85 only two stalagmite high-resolution climate records available from the SE US region covering
86 the Holocene time interval; one from Alabama spanning from 6 ka to ~1 ka BP (Aharon and
87 Dhungana, 2017) and another from West-Central Florida, spanning from 6.6 ka to 4.6 ka BP
88 (Pollock et al., 2016). These high-resolution records reveal novel information about decadal and
89 multidecadal hydroclimate variability in the SE US but do not span the critical YD, 8.2 ka, and
90 LIA cooling intervals to enable assessing the regional impact of ocean thermohaline shifts.

91 In this study we present a hydroclimate record based on stalagmite $\delta^{18}O$ and $\delta^{13}C$ timeseries
92 from the SE US that span the last ~12 ka and allow us to examine subtropical climate responses
93 to high-latitude climate change forced by thermohaline circulation shifts. There is an interest in
94 determining the actual geographical extent of the YD, 8.2 ka and LIA events beyond the circum-
95 North Atlantic region, especially if climate proxy records representing these events are to be
96 used in helping validate models of thermohaline circulation shifts, in the context of potential
97 changes in deep water formation during the Anthropocene (Collins et al., 2019).
98
99

2. Methods

2.1. Study Area

In 2017 we retrieved an inactive stalagmite specimen (34 cm long) named War Eagle (WE) from an isolated cave chamber within War Eagle (WE) cave located in Jackson County, Alabama (Fig. 1 and Fig. S1). This cave is located on private property and is only accessible for half a year, when hunting season is off. WE cave has only one entrance requiring a 41m rappel. The cave is hosted within the Bangor Limestone and the thickness of the epikarst where the stalagmite was found is estimated to be between 30 and 35 m. The soil on the cave's exterior surface is scarce and the topography is categorized as stony colluvial, rockland limestone, and rockland sandstone (United States Department of Agriculture).

2.2. Local and regional climatology

Mean annual precipitation in the locality of WE Cave is 1,446 mm and mean annual temperature is 15°C (1981-2010, NOAA's weather station in Scottsboro, AL., 34.6736N, 86.0536W). Precipitation shows almost no seasonality, with the lowest monthly rainfall amount typically observed in the month of October and the highest in December (Fig. S2). Monthly temperature variations range from the lowest in January (4°C) to the highest in July (26°C) (ncdc.noaa.gov). Alabama like many other locations in the interior southeast has nearly the same amount of precipitation in the warm season as in the cool season. Regional winter precipitation amount comprises the largest portion of the annual budget (29%), followed by spring and summer (~25% each) and lastly fall (~20%) (data from 2005 to 2015). Despite these long-term averages, in recent years summer precipitation has often been greater than other seasons (data

122 from Tuscaloosa, Alabama, 2005-2015) (Dhungana and Aharon, 2019; Lambert and Aharon,
123 2010).

124 Spatial correlation analyses of the instrumental record of monthly precipitation (from
125 1901 to 2013) across the SE US, Caribbean and Gulf of Mexico regions relative to the
126 precipitation record from Alabama, suggest coherent in-phase variability within much of the SE
127 US, and a weak anticorrelation with precipitation variability in the broader Caribbean region
128 (Fig. 1). Anticorrelation reflects the underlying climate dynamics driving seasonal precipitation
129 variability in these regions. Minor precipitation seasonality characterizes the SE US, whereas
130 monsoonal-style seasonality is typical in the broader Caribbean (Karmalkar et al., 2011). End of
131 21st century climate projections suggest contrasting climate responses of these regions as
132 radiative forcing from greenhouse gases increases (Collins et al., 2013).

133 The spatial and temporal pattern of summer precipitation in the SE US is influenced by
134 convective systems (Baigorria et al., 2007), synoptic-scale systems such as tropical cyclones ,
135 and large-scale circulation changes (e.g. (Li et al., 2013) and references therein). During the
136 spring and winter seasons mid-latitude cyclones advect moisture from the Gulf of Mexico and
137 North Atlantic into this region (Keim, 1996). The subtropical North Atlantic ocean, the Mexican
138 Caribbean and the Gulf of Mexico regions represent the main source of year-round moisture for
139 precipitation in large areas of the continental US and particularly of the SE US (Gimeno et al.,
140 2012). Li et al., (2013), examining multiple reanalysis datasets find that the North Atlantic
141 Subtropical High western ridge position is a primary regulator of interannual variation of
142 moisture transport to the SE US and that dynamical processes (atmospheric circulation) are the
143 main control on interannual variations in precipitation.
144

2.3. Cave Monitoring

WE cave monitoring was established in order to better understand cave environmental conditions, particularly temperature and relative humidity; both factors affect the isotopic fractionation between drip water and stalagmite calcite. Two ONSET-HOBO instruments were placed inside the chamber where the WE stalagmite was retrieved, from October 2018 to October 2019. Monitoring results indicate WE cave remained at or near saturation conditions (RH 100%) and was thermally stable year-round with a constant temperature of 14.7°C, thus very close to local mean surface air temperature. These conditions favor isotopic equilibrium between calcite and drip water. Observed cave air thermal stability indicates that it is in thermal equilibrium with outside air temperature and thus responds to persistent air surface temperature change and not seasonal variability. We collected water at one drip site over the course of one year (i.e. from October 2018 to October 2019). Two six-month cumulative water samples yielded the same isotopic values ($\delta^{18}O$= -5.9 ‰) similar to the amount-weighted $\delta^{18}O$ composition of rainfall typically observed in Tuscaloosa (more details below). This indicates that drip water integrates several months and likely more than one year of precipitation amount and that surface and cave evaporative processes are not expected to significantly alter drip water $\delta^{18}O$, similar to what it is observed in a cave in the Yucatan Peninsula, across the Gulf of Mexico (Lases-Hernández et al., 2019) .

2.4. Chronology

The WE stalagmite time scale was determined with 22 U/Th dates (Table S1 and Fig. S3), following the methods by (Cheng et al., 2013). Calcite powders weighing 50 to 130 mg were combined with a calibrated ^{229}Th-^{233}U-^{236}U tracer solution, dissolved, and purified through iron

co-precipitation and anion exchange columns based on the methods of Edwards et al (1987) (Edwards et al., 1987). U-Th isotopic measurements were conducted on a Nu Plasma II-ES multi-collector inductively coupled plasma mass spectrometer (MC-ICP-MS) at the Massachusetts Institute of Technology. Analyses were conducted in static mode, with the minor isotopes (^{234}U and ^{230}Th) measured on a secondary electron multiplier, and all other isotopes measured on Faraday cups. U analyses were bracketed by analyses of standard CRM112a, and Th analyses were bracketed by an in-house ^{229}Th-^{230}Th-^{232}Th standard. All dates are corrected for instrument background, tailing, mass bias, SEM yield, contributions from impurities in the spike, and chemistry blanks using an offline data reduction procedure. All errors of isotopic data and dates given are two standard deviations. Age uncertainties ranged from ±15 to ±110 years with a mean of ±40 years. Only one date has an uncertainty of ±110 years and the remaining 16 dates have uncertainties lower than ±70 years, across the 12 ka record.

U-Th dates indicate that WE stalagmite grew over three time intervals separated by two hiatuses. The stalagmite began to grow 12.2 ka BP and stopped growing at 10.8 ka BP. After an interruption of over 1 ka, the stalagmite resumed growth 9.4 ka BP and stopped growing 4.3 ka BP. Finally, after a ~ 2 ka growth interruption, the stalagmite resumed growth once again 2.6 ka BP and stopped growing 300 years BP (years BP are relative to C.E. 1950). These two hiatuses are visually distinctive as a shift in color, fabric and vertical growth orientation (Fig. S1 & S4). Importantly, the stalagmite spans the intervals of interest corresponding to the YD and 8.2 ka cooling events and the LIA. We developed the chronology of these sections based on piecewise-linear models to account for non-linearity in stalagmite growth (Fig. S3).

2.5. $\delta^{18}O$ & $\delta^{13}C$ Time Series

The $\delta^{18}O$ and $\delta^{13}C$ data was obtained at the Paleoclimate and Stable Isotope Laboratory (PSI) in the Department of Geosciences at Auburn University, Alabama. Along the main growth axis, 688 calcite powder micro samples were drilled at a sampling resolution of 500 μm (Table S2). The carbon and oxygen isotopic composition of calcite powders were analyzed with a Thermo Scientific Delta V Plus Isotope Ratio Mass Spectrometer interfaced with a Thermo Gasbench II. Long-term (3-year) reproducibility for reference standard IAEA-603 is 0.09‰ and 0.07‰ for $\delta^{18}O$ and $\delta^{13}C$, respectively. Reproducibility of $\delta^{18}O$ and $\delta^{13}C$ (average standard deviation for each sample of the WE data-set) were 0.06‰ for both.

3. Results and Discussion

The WE stalagmite long-term average $\delta^{18}O$ composition is -3.3 ‰, with a range from -4.3‰ to -2.1 ‰. The most negative isotopic values occur over the intervals 11.8-11ka BP, 9.4-8 ka BP and 0.5-1 ka BP and the most positive over the intervals 6.5-5.5 ka BP and 10.8-11 ka BP (Fig. 2). We focus this section on the climate interpretation of four separate windows of the WE stalagmite $\delta^{18}O$ record, which span the YD and 8.2 ka cooling events, the Early to Mid-Holocene and the Late Holocene. We provide a final discussion on the WE stalagmite $\delta^{13}C$ series in support of hydroclimate inferences from the $\delta^{18}O$ record.

3.1. Precipitation $\delta^{18}O$ variability and the amount effect

The amount effect is well documented within tropical to subtropical regions (Rozanski et al., 1993) but has not been well documented within the SE US, although modeling data with isotope tracers suggest its existence in the southernmost extension of this region (Vuille et al., 2003).

214 Relevant studies by Dhungana and Aharon (2019) and Lambert and Aharon (2010) suggested the
215 existence of an amount effect on interannual timescales by examining a couple of years of
216 rainfall isotopic data.

217 We examined a 10-year record (2005-2015) of precipitation amount and $\delta^{18}O$ data produced
218 by the University of Alabama (Dhungana and Aharon, 2019; Lambert and Aharon, 2010; McKay
219 and Lambert, 2015) in order to investigate the existence of an amount effect on seasonal and
220 interannual time scales and the impact of shifts in seasonality on precipitation amount and
221 annual precipitation $\delta^{18}O$ (Fig. S5 and Table S3).

222 Examination of decadal precipitation amount (P) and precipitation $\delta^{18}O$ (δP) data (2005-
223 2015), reveals the existence of an interannual relationship between δP and ΔP with a slope
224 $\delta P/\Delta P$ = -0.0017 ‰ per mm) (r=0.34) (Fig. S5A). Removal of three "anomalous" years suggests
225 a much stronger relationship ($\delta P/\Delta P$= -0.003 ‰ per mm) (r=0.92) (Fig. S5B). The observed
226 relationship between precipitation $\delta^{18}O$ and precipitation amount on interannual timescales is the
227 result of an amount effect observed during the summer and spring seasons (hereafter jointly
228 referred to as 'summer') combined with the distinctive depleted isotopic contribution of fall and
229 winter precipitation (hereafter referred to as 'winter'). Although instrumental observations
230 support interpretation of interannual stalagmite $\delta^{18}O$ variability in terms of precipitation amount
231 change, the observed variability of the slope $\delta P/\Delta P$ (i.e. Fig. S5A versus S5B) is significant
232 enough to introduce uncertainty in quantitative precipitation estimates determined *sensu* Medina-
233 Elizalde and Rohling (2012). In this study, we interpret stalagmite $\delta^{18}O$ variability to reflect
234 precipitation amount qualitatively, although we examine the shift in 'winter' and 'summer'
235 precipitation amount using the instrumental data necessary to explain stalagmite $\delta^{18}O$ variability.

An observation from the instrumental record relevant to support hydroclimate interpretations of stalagmite $\delta^{18}O$, is that 'winter' precipitation shows low interannual $\delta^{18}O$ variability, the highest frequency of depleted $\delta^{18}O$ values, and no amount effect on interannual timescales. An amount effect on interannual timescales is particularly observed during the summer and spring seasons (Fig. S6). In order to interpret WE stalagmite $\delta^{18}O$ variability, we examine the effect of shifting the amount of precipitation during 'summer', relative to modern conditions, on the decadal average $\delta^{18}O$ composition of rainfall, while maintaining 'winter' precipitation amount constant, and vice versa, the effect of shifts in 'winter' precipitation on rainfall $\delta^{18}O$ while keeping 'summer' precipitation constant (Fig. 3 and Table S3). We explore decadal rainfall isotopic shifts because this time resolution is relevant to that of the WE stalagmite isotopic records (i.e. 7-44 years) (Fig. 2).

This analysis provides three main observations relevant to the hydroclimate interpretation of stalagmite $\delta^{18}O$: (i) a large increase in 'winter' precipitation amount does not produce *per se* a negative annual precipitation $\delta^{18}O$ shift, but only via dilution of isotopically enriched 'summer' precipitation (Fig. 3). A doubling of 'winter' precipitation amount, for instance, would only shift the decadal average $\delta^{18}O$ composition of rainfall by -0.24‰ when maintaining 'summer' precipitation unchanged (Fig. 3). (ii) Peak negative decadal isotopic shifts can only be attained if 'summer' precipitation increases. This is the result of the amount effect observed during the summer and spring seasons (Fig. S6). Doubling of 'summer' precipitation amount would shift decadal average rainfall $\delta^{18}O$ by -1.4‰, while doubling 'winter' precipitation amount would only shift it by -0.24‰, as mentioned above (Fig. 3). (iii) Maximum positive decadal rainfall isotopic shifts can only be attained by decreasing both 'winter' and 'summer' precipitation. Decreasing 'summer' precipitation amount alone can produce a maximum positive shift of

~+0.21‰ when precipitation is reduced by 48%. A larger 'summer' precipitation reduction starts shifting rainfall $\delta^{18}O$ in the opposite direction, by enhancing the influence of isotopically depleted 'winter' rainfall on the annual isotopic budget. Maximum decline of 'winter' precipitation to zero, produces a decadal averaged positive rainfall isotopic shift of +0.85‰ (Fig. 3). This shift corresponds to the difference between the decadal averaged annual amount-weighed $\delta^{18}O$ composition of rainfall (including all seasons) versus the decadal averaged 'summer' amount-weighed $\delta^{18}O$ composition of rainfall.

3.2. Expected equilibrium stalagmite $\delta^{18}O$ values

A necessary condition to interpret the oxygen isotopic composition of stalagmite calcite as a record of precipitation $\delta^{18}O$ variability is that calcite $\delta^{18}O$ is precipitated under isotopic equilibrium conditions. Results from calculations using empirical isotopic equilibrium equations indicate calcite precipitated at or near equilibrium under the observed cave air temperature (14.7°C) and range of annual amount-weighted $\delta^{18}O$ composition of rainfall (i.e. -5.9 ‰ to -3.9 ‰) would have a $\delta^{18}O$ composition ranging from -6.6 ‰ to -2.9 ‰ in agreement with the WE stalagmite isotopic composition (Table S4). Supported by these results, in addition to the observed cave environmental conditions (relative humidity ~100% and stable temperature), we suggest that stalagmite WE calcite was precipitated near isotopic equilibrium conditions and likely faithfully records precipitation $\delta^{18}O$ variability (Table S4). We note finally that WE stalagmite does not have distinctive temporal laminations to produce a conventional Hendy Test .

3.3. Younger Dryas and 8.2 ka cooling events

Figures 4 and 5 place the WE stalagmite-precipitation $\delta^{18}O$ record in the context of high-latitude climate variability during the YD and 8.2 ka cooling events. Stalagmite $\delta^{18}O$ values become progressively more negative during the evolution of these two events by about ~-1.2‰. The observed relationship between precipitation $\delta^{18}O$ and precipitation amount observed today on interannual timescales suggests that such negative shift in stalagmite $\delta^{18}O$ reflects persistent increases in precipitation amount in the SE US during the peak of these events (Fig. S5). We acknowledge that the negative stalagmite $\delta^{18}O$ shift observed during the YD and 8.2 ka events could reflect regional atmospheric cooling via the same-sign relationship between water condensation temperature and precipitation $\delta^{18}O$. Global circulation model hosing experiments with isotope tracers suggest, however, that precipitation $\delta^{18}O$ would have remained practically unchanged in the SE US (LeGrande et al., 2006). WE cave air cooling during these events, on the other hand, would have increased calcite $\delta^{18}O$ not decrease it, due to thermodynamic isotopic fractionation between drip water and calcite, probably counterbalancing positive rainfall isotopic shifts driven by atmospheric cooling.

The sensitivity test we applied using the instrumental data (Fig. 3) suggests that the stalagmite isotopic shift of ~-1.2‰ can be explained by a 90% increase of 'summer' precipitation relative to today's conditions. As mentioned previously, an increase in 'winter' precipitation by 100% would only shift rainfall $\delta^{18}O$ by -0.2 ‰ (while maintaining 'summer' precipitation amount constant). We cannot discard that 'winter' precipitation declined at the time, because such a large increase in the influence of 'summer' precipitation would mask the isotopic signal of declining 'winter' rainfall amount. As an example, a coeval decrease of 'winter' precipitation amount by 100% would only shift rainfall $\delta^{18}O$ by -0.1‰ when 'summer'

305 precipitation increases 90% (Table S3). We point out that a decrease of 'summer' precipitation to
306 zero while maintaining 'winter' precipitation unchanged would decrease rainfall $\delta^{18}O$ only by a
307 maximum of -0.7‰ and thus would fail to explain the observed stalagmite isotopic change of -
308 1.2‰. An increase in 'summer' precipitation is thus necessary to explain observations. We lastly
309 note that the suggested increase in 'summer' precipitation by 90% yields an increase in annual
310 precipitation, even when winter precipitation amount is reduced by as much as 90%; in
311 agreement with inferences based on the observed amount effect on interannual timescales (Fig.
312 S6).

313 The YD and 8.2 ka events were associated with AMOC slowdown, North Atlantic
314 cooling, a southward displacement of the ITCZ, and precipitation reductions in the NH low
315 latitudes as suggested by climate model hosing experiments (Dahl et al., 2005; LeGrande et al.,
316 2006; Otto-Bliesner and Brady, 2010; Vellinga and Wood, 2002) and paleoclimate records (Lea
317 et al., 2003; Peterson and Haug, 2006). A southward displacement of the ITCZ during the YD
318 and 8.2 ka events in particular is suggested by the Cariaco Basin Ti% sediment record from
319 offshore Venezuela and from its antiphase relationship with hydroclimate records from south
320 America (Peterson and Haug, 2006) (Figs. 4 and 5). A southward displacement of the ITCZ due
321 to AMOC slowdown is also supported by climate model simulations and expected to result from
322 atmospheric circulation changes associated with significant tropical cooling (Otto-Bliesner and
323 Brady, 2010; Stouffer et al., 2006; Vellinga and Wood, 2002).

324 Model simulations of AMOC slowdown/shutdown feature a 'cold tongue' of surface
325 temperatures that extends from the North Atlantic high-latitudes through the eastern North
326 Atlantic sector down to the tropical region (Otto-Bliesner and Brady, 2010; Vellinga and Wood,
327 2002). This ocean 'cold tongue' is flanked by mild or warmer surface temperatures in the

western North Atlantic mid-latitude and Gulf of Mexico regions, the main sources of moisture into the SE US region (Gimeno et al., 2012; Li et al., 2013). Additional model hosing experiments that address shifts in seasonality (LeGrande et al., 2006; Renssen et al., 2002), suggest that AMOC slowdown decreases winter surface temperatures while summer temperatures remain unchanged or increase in the Gulf of Mexico and SE US. Warmer ocean conditions in the Gulf of Mexico and western North Atlantic, particularly in the summer, coeval with stronger meridional and zonal temperature gradients in the North Atlantic would be conducive to increasing local precipitation in the SE US. Enhanced precipitation in the SE US is actually supported by various model experiments of freshwater perturbation to AMOC that at the same time simulate coeval precipitation reduction in the tropical Atlantic (LeGrande et al., 2006; Renssen et al., 2002; Vellinga and Wood, 2002), in agreement with observations (Fig. 4 and 5). We acknowledge that these observations have potential implications for the inferred position and strength of the North Atlantic subtropical high pressure system during these climate events that deserve a deeper exploration beyond the scope of this study.

The results from this study suggesting the SE US was wet when the North Atlantic was cold and the tropics experienced negative precipitation anomalies agree with independent paleoclimate evidence based on pollen and plant macrofossil records from Lake Tulane, Florida. These records spanning the last 60 ka suggest that Florida was wet and warm during Heinrich events, including the YD, and during the stadial intervals of Dansgaard-Oeschger events (Grimm et al., 2006). Grimm et al., (2006) suggest that a reduction in North Atlantic deep water formation decreased the northward ocean heat transport and retained warmth in the subtropical Atlantic and Gulf of Mexico, essentially producing a polar-subtropical seesaw. Paleoclimate evidence both supporting and opposing the seesaw pattern exists from the Caribbean, as

351 described in detail by Grimm et al. (2006). Regardless of the mechanism ultimately enhancing
352 summer precipitation in the SE US, model simulations and paleoclimate records provide
353 evidence of an antiphase climate relationship between the SE US and the eastern subtropical
354 North Atlantic and southern Caribbean, during events of AMOC slowdown/shutdown. We note
355 that the instrumental record indicates an antiphase relationship between precipitation in the SE
356 US and the broader Caribbean on interannual timescales (Fig. 1) and during the summer season
357 (Fig. S7).
358
359 *3.5. Early to Mid-Holocene Climate Variability*
360 The WE stalagmite suggests a long-term +1‰ isotopic shift occurring from ~ 7.5 ka to ~5.5
361 ka (Fig. 6). A decline in 'summer' precipitation alone would not explain this large positive
362 isotopic shift, because it would increase $\delta^{18}O$ by +0.2‰ maximum, when precipitation amount
363 decreases by 49% (Fig. 3). As mentioned previously, a decrease of 'summer' precipitation
364 amount beyond this level would no longer increase annual precipitation $\delta^{18}O$ because the
365 depleted isotopic composition of 'winter' rainfall becomes dominant after this threshold (Fig. 3).
366 An additional 75% decline of 'winter' precipitation amount would be needed to explain the Mid-
367 Holocene stalagmite positive isotopic shift. We note that 'summer' precipitation must have
368 declined together with 'winter' precipitation, because the maximum isotopic shift when 'winter'
369 precipitation becomes zero is 0.8‰, therefore it would still be insufficient to explain the mid-
370 Holocene stalagmite shift (Fig. 3). The precipitation decline from ~7 to ~6 ka suggested by the
371 WE stalagmite is consistent with pollen records from wetlands in the SE US that suggest a
372 decline over this time of high-diversity taxa indicative of moist soils (Goman and Leigh, 2004).
373 In addition, a hydroclimate transition from wet to dry conditions at the time is also suggested by

374 a decrease in the abundance of *Pinus* inferred from pollen records from lake Tulane, Florida
375 (Grimm et al., 1993; Grimm et al., 2006).
376 Inferred climate evolution from the Early Holocene (9-7 ka BP) to the mid-Holocene (6-5 ka
377 BP) in the SE US coincides with boreal summer insolation reduction , North Atlantic cooling
378 (Marcott et al., 2013; Renssen et al., 2005; Wanner et al., 2011), decrease rainfall in the
379 Caribbean (Haug et al., 2001) and weakening of Northern Hemisphere monsoon intensity
380 (Fleitmann et al., 2007) (Fig. 6). Evidence of mid-Holocene precipitation reduction is also
381 provided by paleoclimate records from Cuba (Fensterer et al., 2013), and from the central and
382 northwestern US (Shin et al., 2006). Lastly, Early Holocene precipitation maxima in the SE US
383 coeval with Northern Hemisphere warm conditions is consistent with projected hydroclimate
384 change in the region by the end of this century resulting from anthropogenic warming (Collins et
385 al., 2013).
386 The drying trend suggested by the WE stalagmite is interrupted by two climate reversals
387 between 6 and 4.5 ka BP indicated by prominent negative isotopic excursions (Fig. 2 and Fig.
388 S8). These inferred climate reversals are also represented, although more subtlety, by the
389 stalagmite $\delta^{18}O$ record from DeSoto Caverns, Alabama, that spans the interval between ~6 ka
390 and 1 ka BP (Aharon and Dhungana, 2017) (Fig. S8). Similar but more subtle hydroclimate
391 cycles are shown by paleoclimate records from the Caribbean which are coeval with North
392 Atlantic temperature variability (Haug et al., 2001; Marcott et al., 2013)(Fig. 5). Isotopic
393 reversals are observed in the WE stalagmite $\delta^{13}C$ record, also suggesting a local hydrological
394 change at the time (Fig. 2). We propose that the speleothem isotopic records from Alabama
395 probably record an amplified regional hydrological response to North Atlantic climate conditions
396 perhaps reflecting that dynamical processes became progressively less influential in controlling

moisture sources into the SE US from the early to the mid-Holocene. During this time, the region began to experience an increase in precipitation recycling from precipitation of terrestrial origin (Dominguez et al., 2006) that became more important as oceanic sources of moisture became less dominant as the North Atlantic cooled (Gimeno et al., 2012; Li et al., 2013).

3.6. Late-Holocene Climate Variability

During the transition from the Medieval Climate Anomaly time interval to the Little Ice Age (Mann et al., 2009), WE stalagmite $\delta^{18}O$ shows a negative isotopic shift from 1.2 to 0.4 ka BP of ~-0.8‰ (Fig. 7). The stalagmite negative isotopic excursion coincides with the LIA interval (Mann et al., 2009); arguably the Holocene's coldest period in the North Atlantic (Marcott et al., 2013) and the driest in the Caribbean (Higuera-Gundy et al., 1999; Hodell et al., 1991; Peterson and Haug, 2006). Similar to our interpretation concerning the YD and 8.2 ka events, we suggest this negative isotopic excursion reflects an increase in 'summer' precipitation. Tree ring records from the eastern SE US spanning the last 1000 years (Stahle and Cleaveland, 1992) do not suggest a long-term shift in spring precipitation during the LIA interval. Thus, the long-term stalagmite isotopic shift associated with the LIA is likely to reflect mostly summer precipitation changes during this time. Climate variability in the SE US across the YD, 8.2 ka, and LIA events support a connection with AMOC shifts (Keigwin and Boyle, 2000; Lund et al., 2006); in the case of the LIA, perhaps reflecting ocean-atmospheric feedbacks to forcing from volcanic sulfur emissions and total solar irradiance at the time (Andres and Peltier, 2016; Free and Robock, 1999).

3.7. Stalagmite Carbon Isotopes

Across the full length of the WE stalagmite, and during the prominent climate events highlighted above, the stalagmite $\delta^{13}C$ record mimics the oxygen isotope record (Fig. 2). The carbon isotope response across these events suggests hydrological shifts affecting vegetation type, density, and/or soil microbial productivity. We note that most of the stalagmite $\delta^{13}C$ record have values that suggest a strong dominance of carbon of bedrock origin with positive isotopic compositions and only minor contributions of carbon from vegetation dominated by C4 plants (Fairchild and Baker, 2012). We therefore conclude that stalagmite calcite covariance between $\delta^{18}O$ and $\delta^{13}C$ probably reflects shifts in karst hydrology whereby wetter conditions would favor faster infiltration, decreased pCO_2 degassing and reduced prior calcite precipitation, ultimately producing lower $\delta^{13}C$ values from a bedrock-dominated carbon baseline (Fairchild and Baker, 2012).

4. Conclusion

We produced high-resolution stalagmite $\delta^{18}O$ and $\delta^{13}C$ records of hydroclimate from Alabama spanning the last 12 ka, extending the existing regional paleoclimate record to the early Holocene. Hydroclimate in Alabama is linked to the broader Southeastern United States (SE US) as suggested by spatial correlation analysis using the instrumental record of precipitation amount. We interpret the stalagmite isotope records to reflect: (i) an amount effect observed on interannual timescales, and; (ii) shifts in the relative contribution of changes in spring-summer versus fall-winter rainfall amount. We find a close connection between hydroclimate variability in the SE US, North Atlantic high latitude climate variability and Caribbean/Gulf of Mexico hydroclimate. A consistent picture emerges whereby spring-summer precipitation in the SE US

443 increases during events of high latitude cooling associated with Atlantic Meridional Circulation
444 slowdown/shutdown, such as during the Younger Dryas, 8.2 ka and Little Ice Age cooling
445 events. Speleothem evidence of hydroclimate change is supported by pollen records from Florida
446 and shows consistency with climate model studies of AMOC slowdown/shutdown. WE
447 speleothem isotopic records suggest that annual precipitation decreased in the SE US across the
448 climate transition from the early Holocene ('Holocene Climate Optimum') to the late Holocene
449 (the 'Neoglacial') in the Northern Hemisphere, generally attributed to external orbital forcing.
450 Results from this study have implications for our understanding of the sensitivity of subtropical
451 North Atlantic hydroclimate to abrupt melting of the Greenland ice sheet and its influence on
452 AMOC in a future dominated by increasing greenhouse gases.
453
454 Acknowledgments
455 We are specially thankful to Mr. Milton Polsky, War Eagle cave land owner, for allowing us to
456 access the cave and for his support during fieldwork. We offer special thanks also to Dr. Rajesh
457 Dhungana for providing the rainfall isotopic data collected at the University of Alabama by Katie
458 McKay and Dr. Joe Lambert. We thank Dr. Joe Lambert and Prof. Raymond Bradley for
459 providing valuable comments that helped improve this manuscript. Support to this project came
460 from Prof. Medina's startup funding from Auburn University.
461
462 **Figure Captions**
463 Figure 1. Spatio-temporal correlation analysis of precipitation (monthly values from 1901 to
464 2013 and with a spatial coverage of 0.5° latitude by 0.5° longitude) at the location (34°31′N,
465 86°11′W) (War Eagle Cave, Alabama). Location of War Eagle Cave indicated with light blue
466 star. The precipitation data set comes from the GPCC Global Precipitation Climatology Centre

and is available from https://psl.noaa.gov/data/gridded/data.gpcc.html. The map was created using the R software .

Figure 2. Stalagmite War Eagle (WE) $\delta^{18}O$ and $\delta^{13}C$ records spanning the last 12.2 ka. Vertical colored bars indicate relevant time intervals discussed in the manuscript. The time resolution of these records is from 7 to 44 years, decreasing as time progresses from the Early to the Late Holocene.

Figure 3. Plot illustrating the change in the decadal average $\delta^{18}O$ composition of rainfall resulting from shifting the amount of precipitation during spring and summer labelled as 'summer', and fall and winter, labeled as 'winter', relative to modern conditions. The X axis represents the fractional change in precipitation amount from modern conditions; 1= 100% increase or a doubling of precipitation amount, and -1=100% decline in precipitation amount. *Blue line* represents the expected decadal average $\delta^{18}O$ composition shift from changing the amount of precipitation during 'winter' from -100% (no precipitation) to plus 100% (doubling) while keeping 'summer' precipitation amount constant. *Dark orange line*, represents the expected decadal average $\delta^{18}O$ composition shift from changing the amount of precipitation during 'summer' keeping 'winter' precipitation amount constant. These calculations include the amount effect relationship during the summer and spring seasons observed today.
A decrease in 'summer' precipitation increases the decadal average $\delta^{18}O$ composition of rainfall, because of the inverse relationship between precipitation amount and precipitation $\delta^{18}O$ during the summer and spring, up to the point when the decline of 'summer' precipitation amount and its relatively positive isotopic composition "enhances" the influence of the depleted isotopic

490 composition that characterizes ‘winter’ precipitation (shown in plot section as “ ‘winter’ isotopic
491 composition dominates”). The maximum positive isotopic shift produced from a reduction in
492 ‘summer’ precipitation amount *per se*, keeping ‘winter’ precipitation constant, is 0.21‰
493 associated with a 40% precipitation amount reduction. A larger decrease in ‘summer’
494 precipitation amount no longer increases the isotopic composition of rainfall, because as
495 mentioned above the depleted isotopic composition of winter begins to dominate. On the other
496 hand, because there is no relationship between precipitation amount and precipitation $\delta^{18}O$
497 during ‘winter’ and there is an amount effect during summer, an increase in ‘winter’
498 precipitation has a much modest effect that an increase in ‘summer’ precipitation amount on
499 rainfall $\delta^{18}O$. A doubling in the amount of ‘winter’ precipitation is expected to decrease the
500 decadal average $\delta^{18}O$ composition of rainfall by 0.24‰, whereas a doubling in ‘summer’
501 precipitation amount would decrease the $\delta^{18}O$ of rainfall by 1.4‰.
502
503 Figure 4. Blow up comparing the NGRIP ice core $\delta^{18}O$ record (panel A) (Rasmussen et al.,
504 2006), the Ti% record from the Cariaco Basin, offshore Venezuela (panel B) (Haug et al., 2001)
505 and the WE stalagmite $\delta^{18}O$ record (panel C, this study) over the Younger Dryas time interval.
506 Note that top X-axis representing panels A and B and the bottom X-axis representing panel C,
507 are shifted relative to each other with a maximum offset of ~200 yrs, in order to accommodate a
508 dating uncertainty in the layer counting of young ice of ±120 yrs in the NGRIP ice core record
509 (Rasmussen et al., 2006) and in the stalagmite $\delta^{18}O$ record ~12 ka BP of ± 70 yrs (Table S1).
510 Top X-scale corresponds to that of the records presented on panels A and B and the bottom X-
511 scale corresponds to the WE stalagmite record.
512

513 Figure 5. Blow up comparing the NGRIP ice core $\delta^{18}O$ record (panel A) (Rasmussen et al.,
514 2006), the Ti% record from the Cariaco Basin, offshore Venezuela (panel B) and the WE
515 stalagmite $\delta^{18}O$ record (panel C, this study) over the 8.2 ka cooling event.
516
517 Figure 6. Blow up comparing a North Atlantic sea surface temperature reconstruction (panel A)
518 (Marcott et al., 2013), the Cariaco Basin Ti% record (panel B) (Haug et al., 2001) and the WE
519 stalagmite $\delta^{18}O$ record (panel C, this study) spanning the transition from the Early to the Mid-
520 Holocene. Darker continuous lines represent 7-point moving averages.
521
522 Figure 7. Blow up comparing a Northern Hemisphere surface temperature record (panel
523 A)(Mann et al., 2009), the Cariaco Basin Ti% record (panel B) (Haug et al., 2001) and the WE
524 stalagmite $\delta^{18}O$ record (panel C, this study) spanning the late Holocene. The mean resolution of
525 the stalagmite record over this time interval is 44 yrs.
526
527
528 References
529 1. Aharon, P., and Dhungana, R., 2017, Ocean-atmosphere interactions as drivers of mid-to-
530 late Holocene rapid climate changes: Evidence from high-resolution stalagmite records at
531 DeSoto Caverns, Southeast USA: Quaternary Science Reviews, v. 170, p. 69-81.
532 2. Anandhi, A., and Bentley, C., 2018, Predicted 21st century climate variability in
533 southeastern U.S. using downscaled CMIP5 and meta-analysis: CATENA, v. 170, p. 409-
534 420.
535 3. Andres, H. J., and Peltier, W. R., 2016, Regional Influences of Natural External Forcings
536 on the Transition from the Medieval Climate Anomaly to the Little Ice Age: Journal of
537 Climate, v. 29, no. 16, p. 5779-5800.
538 4. Baigorria, G. A., Jones, J. W., and O'Brien, J. J., 2007, Understanding rainfall spatial
539 variability in southeast USA at different timescales: International Journal of Climatology,
540 v. 27, no. 6, p. 749-760.
541 5. Bard, E., Rostek, F., Turon, J.-L., and Gendreau, S., 2000, Hydrological impact of
542 Heinrich events in the subtropical northeast Atlantic: Science v. 289, p. 1321–1324.

6. Broecker, W. S., Kennett, J. P., Flower, B. P., Teller, J. T., Trumbore, S., Bonani, G., and Wolfli, W., 1989, Routing of meltwater from the Laurentide Ice Sheet during the Younger Dryas cold episode: Nature, v. 341, no. 6240, p. 318-321.
7. Cheng, H., Edwards, R. L., Shen, C.-C., Polyak, V. J., Asmerom, Y., Woodhead, J., Hellstrom, J., Wang, Y., J., , Kong, X. G., Spötl, C., Wang, X. F., and Alexander, E. C., 2013, Improvements in 230Th dating, 230Th and 234U half-life values, and U-Th isotopic measurements by multi-collector inductively coupled plasma mass spectrometry.: Earth and Planetary Science Letters, v. 372, p. 82-91.
8. Collins, M., R. Knutti, R., Arblaster, J., Dufresne, J.-L., Fichefet, T., Friedlingstein, P., and Gao, X., 2013, Long-term Climate Change: Projections, Commitments and Irreversibility: Climate Change 2013: The Physical Science Basis. Contribution of Working Group I to the Fifth Assessment Report of the Intergovernmental Panel on Climate Change
9. Collins, M., Sutherland, M., Bouwer, L., Cheong, S.-M., Frölicher, T., Jacot Des Combes, H., and M. Koll Roxy, I. L., K. McInnes, B. Ratter, E. Rivera-Arriaga, R.D. Susanto, D. Swingedouw, and L. Tibig, 2019, Extremes, Abrupt Changes and Managing Risk: IPCC Special Report on the Ocean and Cryosphere in a Changing Climate.
10. Dahl, K. A., Broccoli, A. J., and Stouffer, R. J., 2005, Assessing the role of North Atlantic freshwater forcing in millennial scale climate variability: a tropical Atlantic perspective: Climate Dynamics, v. 24, no. 4, p. 325-346.
11. Dhungana, R., and Aharon, P., 2019, Stable isotopes and trace elements of drip waters at DeSoto Caverns during rainfall-contrasting years: Chemical Geology, v. 504, p. 96-104.
12. Dominguez, F., Kumar, P., Liang, X.-Z., and Ting, M., 2006, Impact of Atmospheric Moisture Storage on Precipitation Recycling: Journal of Climate, v. 19, no. 8, p. 1513-1530.
13. Edwards, L. R., Chen, J. H., and Wasserburg, G. J., 1987, 238U234U230Th232Th systematics and the precise measurement of time over the past 500,000 years: Earth and Planetary Science Letters, v. 81, no. 2, p. 175-192.
14. Fairchild, J., and Baker, A., 2012, Speleothem Science: from Process to Past Environments, Oxford, Wiley-Blackwell.
15. Fensterer, C., Scholz, D., Hoffmann, D. L., Spotl, C., Schroder-Ritzrau, A., Horn, C., Pajon, J. M., and Mangini, A., 2013, Millennial-scale climate variability during the last 12.5 ka recorded in a Caribbean speleothem: Earth and Planetary Science Letters, v. 361, p. 143-151.
16. Fleitmann, D., Burns, S., Mangini, A., Mudelsee, M., Kramers, J., Villa, I., Neff, U., Al-Subbary, A., Buettner, A., Hippler, D., and Matter, A., 2007, Holocene ITCZ and Indian Monsoon Dynamics Recorded in Stalagmites from Oman and Yemen (Socotra): Quaternary Science Reviews, v. 26, p. 170-188.
17. Free, M., and Robock, A., 1999, Global warming in the context of the Little Ice Age: Journal of Geophysical Research: Atmospheres, v. 104, no. D16, p. 19057-19070.
18. Gimeno, L., Stohl, A., Trigo, R. M., Dominguez, F., Yoshimura, K., Yu, L., Drumond, A., Durán-Quesada, A. M., and Nieto, R., 2012, Oceanic and terrestrial sources of continental precipitation: Reviews of Geophysics, v. 50, no. 4.
19. Goman, M., and Leigh, D., 2004, Wet early to middle Holocene conditions on the Upper Coastal Plain of North Carolina, USA: Quaternary Research, v. 61, p. 256-264.

20. Grimm, E. C., Jacobson, G. L., Watts, W. A., Barbara, C. S. H., and Maasch, K. A., 1993, A 50,000-Year Record of Climate Oscillations from Florida and Its Temporal Correlation with the Heinrich Events: Science, v. 261, no. 5118, p. 198-200.
21. Grimm, E. C., Watts, W. A., Jacobson, G. L., Hansen, B. C. S., Almquist, H. R., and Dieffenbacher-Krall, A. C., 2006, Evidence for warm wet Heinrich events in Florida: Quaternary Science Reviews, v. 25, no. 17, p. 2197-2211.
22. Haug, G. H., Hughen, K. A., Sigman, D. M., Peterson, L. C., and Röhl, U., 2001, Southward Migration of the Intertropical Convergence Zone Through the Holocene: Science, v. 293, no. 5533, p. 1304-1308.
23. Higuera-Gundy, A., Brenner, M., Hodell, D. A., Curtis, J. H., Leyden, B. W., and Binford, M. W., 1999, A 10,300 C-14 yr record of climate and vegetation change from Haiti: Quaternary Research, v. 52, no. 2, p. 159-170.
24. Hodell, D. A., Curtis, J. H., Jones, G. A., Higuera-Gundy, A., Brenner, M., Binford, M. W., and Dorsey, K. T., 1991, Reconstruction of Caribbean climate change over the past 10,500 years: Nature, v. 352, no. 6338, p. 790-793.
25. IPBES, 2019, Summary for policymakers of the global assessment report on biodiversity and ecosystem services of the Intergovernmental Science-Policy Platform on Biodiversity and Ecosystem Services.: IPBES secretariat, Bonn, Germany.
26. Ipcc, 2014, Climate Change 2014: Impacts, Adaptation, and Vulnerability. Part A: Global and Sectoral Aspects. Contribution of Working Group II to the Fifth Assessment Report of the Intergovernmental Panel on Climate Change [Field, C.B., V.R. Barros, D.J. Dokken, K.J. Mach, M.D. Mastrandrea, T.E. Bilir, M. Chatterjee, K.L. Ebi, Y.O. Estrada, R.C. Genova, B. Girma, E.S. Kissel, A.N. Levy, S. MacCracken, P.R. Mastrandrea, and L.L. White (eds.)], Cambridge, United Kingdom and New York, NY, USA, Cambridge University Press, 1132 p.:
27. Karmalkar, A. V., Bradley, R. S., and Diaz, H. F., 2011, Climate change in Central America and México: regional climate model validation and climate change projections: Climate Dynamics, v. 37, p. 605-629.
28. Keigwin, L. D., and Boyle, E. A., 2000, Detecting Holocene changes in thermohaline circulation: Proceedings of the National Academy of Sciences, v. 97, no. 4, p. 1343-1346.
29. Keim, B., 1996, Spatial, synoptic, and seasonal patterns of heavy rainfall in the Southeastern United States: Physical Geography, v. 17, p. 313-328.
30. Lambert, J. W., and Aharon, P., 2010, Oxygen and hydrogen isotopes of rainfall and dripwater at SeSoto Caverns (Alabama, USA); Key to understanding past variability of moisture transport from the Gulf of Mexico: Geochimica Et Cosmochimica Acta, v. 74, no. 3, p. 846-861.
31. Lases-Hernández, F., Medina-Elizalde, M., Burns, S., Bernal-Uruchurtu, J. P., and Beddows, P., 2019, Monitoring Rio Secreto Cave System in the Yucatan Peninsula to Calibrate Paleoclimatic Proxies: Geochimica Et Cosmochimica Acta, v. 246, p. 41-59.
32. Lea, D. W., Pak, D. K., Peterson, L. C., and Hughen, K. A., 2003, Synchroneity of Tropical and High-Latitude Atlantic Temperatures over the Last Glacial Termination: Science, v. 301, no. 5638, p. 1361-1364.
33. LeGrande, A. N., Schmidt, G. A., Shindell, D. T., Field, C. V., Miller, R. L., Koch, D. M., Faluvegi, G., and Hoffmann, G., 2006, Consistent simulations of multiple proxy responses to an abrupt climate change event: Proceedings of the National Academy of Sciences of the United States of America, v. 103, no. 4, p. 837-842.

34. Li, L., Li, W., and Barros, A. P., 2013, Atmospheric moisture budget and its regulation of the summer precipitation variability over the Southeastern United States: Climate Dynamics, v. 41, no. 3, p. 613-631.
35. Lund, D. C., Lynch-Stieglitz, J., and Curry, W. B., 2006, Gulf Stream density structure and transport during the past millennium: Nature, v. 444, no. 7119, p. 601-604.
36. Mann, M. E., Zhang, Z., Rutherford, S., Bradley, R. S., Hughes, M. K., Shindell, D., Ammann, C., Fluvegi, G., and Ni, F., 2009, Global Signatures and Dynamical Origins of the Little Ice Age and Medieval Climate Anomaly: Science, v. 326, p. 1256-1260.
37. Marcott, S. A., Shakun, J. D., Clark, P. U., and Mix, A. C., 2013, A Reconstruction of Regional and Global Temperature for the Past 11,300 Years: Science, v. 339, no. 6124, p. 1198-1201.
38. Matthes, F., 1939, Report of Committee on Glaciers: Trans. Am. Geophys. Union, v. 20, p. 518-535.
39. McKay, K., and Lambert, W. J., 2015, Utilizing present-say stable water isotopes to improve paleoclimate records from the Southeast (USA), American Geophysical Union: San Francisco, CA
40. Medina-Elizalde, M., Burns, S. J., Polanco-Martinez, J., Lases-Hernández, F., Bradley, R., Wang, H.-C., and Shen, C.-C., 2017, Synchronous precipitation reduction in the American Tropics associated with Heinrich 2: Scientific Reports, v. 7, no. 1, p. 11216.
41. Otto-Bliesner, B. L., and Brady, E. C., 2010, The sensitivity of the climate response to the magnitude and location of freshwater forcing: last glacial maximum experiments: Quaternary Science Reviews, v. 29, p. 56-73.
42. Peterson, L. C., and Haug, G. H., 2006, Variability in the mean latitude of the Atlantic Intertropical Convergence Zone as recorded by riverine input of sediments to the Cariaco Basin (Venezuela): Palaeogeography Palaeoclimatology Palaeoecology, v. 234, no. 1, p. 97-113.
43. Pollock, A. L., van Beynen, P. E., DeLong, K. L., Polyak, V., and Asmerom, Y., 2016, A speleothem-based mid-Holocene precipitation reconstruction for West-Central Florida: The Holocene, v. 27, no. 7, p. 987-996.
44. Rasmussen, S. O., Andersen, K. K., Svensson, A. M., Steffensen, J. P., Vinther, B. M., Clausen, H. B., Siggaard-Andersen, M.-L., Johnsen, S. J., Larsen, L. B., Dahl-Jensen, D., Bigler, M., Röthlisberger, R., Fischer, H., Goto-Azuma, K., Hansson, M. E., and Ruth, U., 2006, A new Greenland ice core chronology for the last glacial termination: Journal of Geophysical Research: Atmospheres, v. 111, no. D6.
45. Renssen, H., Goosse, H., and Fichefet, T., 2002, Modeling the effect of freshwater pulses on the early Holocene climate: The influence of high-frequency climate variability: Paleoceanography, v. 17, no. 2, p. 10-11-10-16.
46. Renssen, H., Goosse, H., Fichefet, T., Brovkin, V., Driesschaert, E., and Wolk, F., 2005, Simulating the Holocene climate evolution at high latitudes using a coupled atmosphere–sea ice–ocean–vegetation model: Climate Dynamics, v. 24, p. 23-43.
47. Rozanski, K., Araguás-Araguás, L., and Gonfiantini, R., Isotopic patterns in modern global precipitation *in* Proceedings Climate Change in Continental Isotopic Records, American Geophisical Union, 1993, Volume 78, Geophysical Monograph
48. Shin, S.-I., Sardeshmukh, P., Webb, R., Oglesby, R., and Barsugli, J., 2006, Understanding the Mid-Holocene Climate: Journal of Climate v. 19.

679 49. Stahle, D. W., and Cleaveland, M. K., 1992, Reconstruction and Analysis of Spring
680 Rainfall over the Southeastern U.S. for the Past 1000 Years: Bulletin of the American
681 Meteorological Society, v. 73, no. 12, p. 1947-1961.
682 50. Stouffer, R. J., Yin, J., Gregory, J. M., Dixon, K. W., Spelman, M., J., Hurlin, W.,
683 Weaver, A. J., Eby, M., Flato, G. M., Hasumi, H., Hu, A., Jungclaus, J. H.,
684 Kamenkovich, I. V., Levermann, A., Montoya, M., Murakami, S., Nawrath, S., Oka, A.,
685 and Peltier, W., 2006, Investigating the Causes of the Response of the Thermohaline
686 Circulation to Past and Future Climate Changes: Journal of Climate: v. 19, p. 1365–1387.
687 51. Thomas, E. R., Wolff, E. W., Mulvaney, R., Steffensen, J. P., Johnsen, S. J., Arrowsmith,
688 C., White, J. W. C., Vaughn, B., and Popp, T., 2007, The 8.2ka event from Greenland ice
689 cores: Quaternary Science Reviews, v. 26, no. 1, p. 70-81.
690 52. Vellinga, M., and Wood, R. A., 2002, Global Climatic Impacts of a Collapse of the
691 Atlantic Thermohaline Circulation: Climatic Change, v. 54, no. 3, p. 251-267.
692 53. Wanner, H., Solomina, O., Grosjean, M., Ritz, S. P., and Jetel, M., 2011, Structure and
693 origin of Holocene cold events: Quaternary Science Reviews, v. 30, no. 21, p. 3109-3123.
694
695

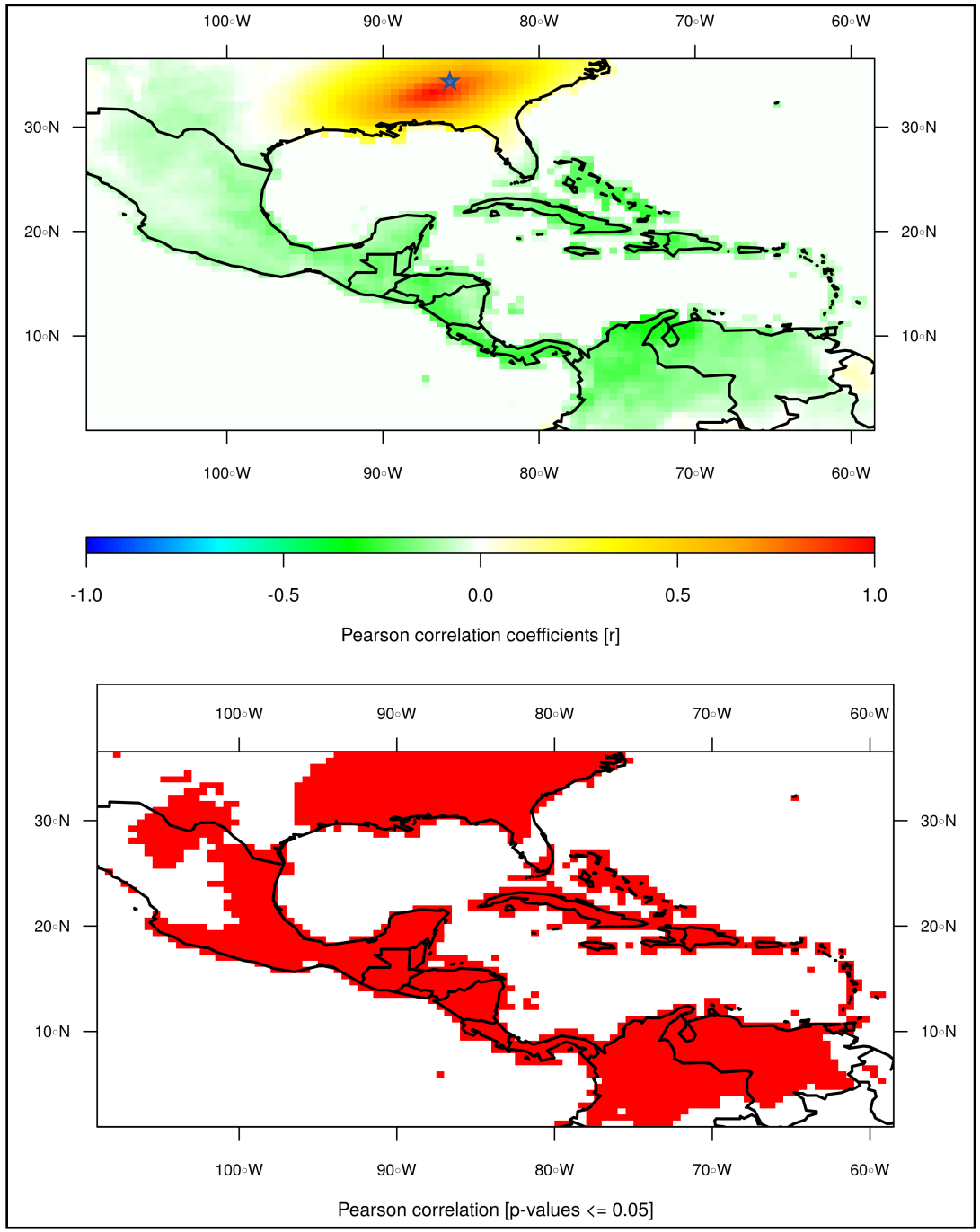
100◦W
90◦W
80◦W
70◦W
60◦W
30◦N
20◦N
10◦N
-1.0
-0.5
0.0
0.5
1.0
Pearson correlation coefficients [r]
Pearson correlation [p-values <= 0.05]

Figure 1.

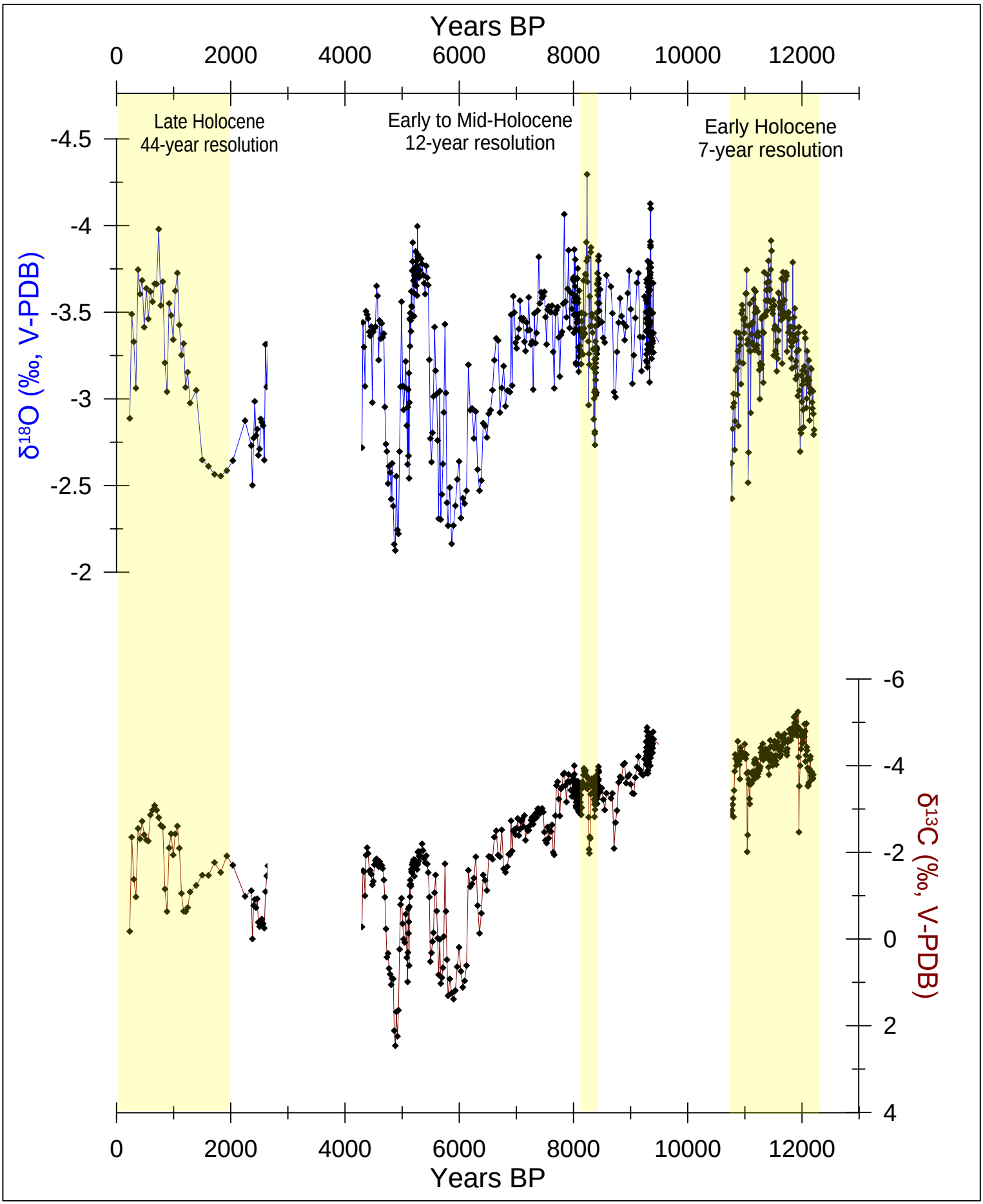
Years BP
0
2000
4000
6000
8000
10000
12000
Late Holocene
44-year resolution
Early to Mid-Holocene
12-year resolution
Early Holocene
7-year resolution
-4.5
-4
-3.5
-3
-2.5
-2
δ18O (‰, V-PDB)
-6
-4
-2
0
2
4
δ13C (‰, V-PDB)
0
2000
4000
6000
8000
10000
12000
Years BP

Figure 2

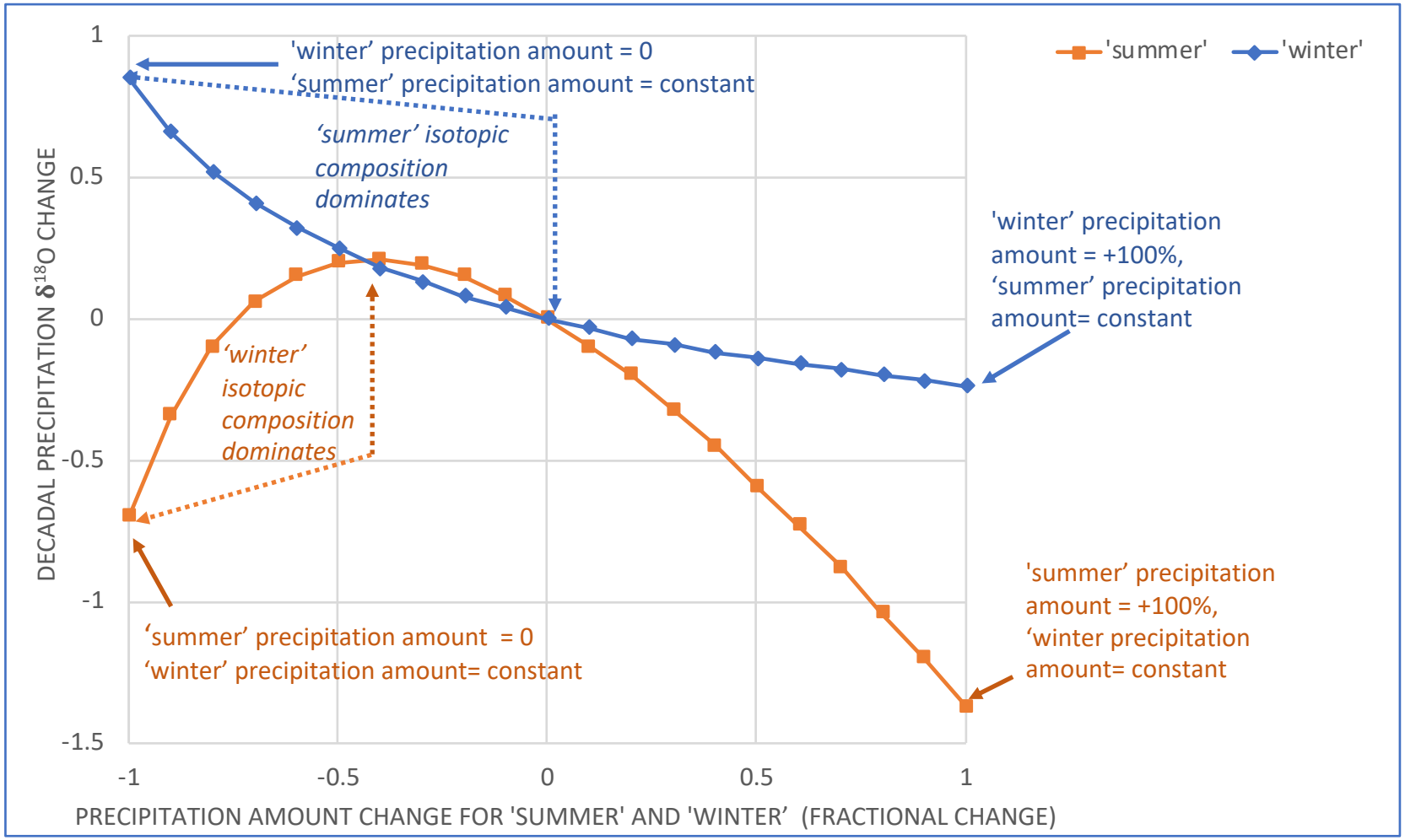
'summer'
'winter'
'winter' precipitation amount = 0
'summer' precipitation amount = constant
'summer' isotopic composition dominates
'winter' precipitation amount = +100%, 'summer' precipitation amount= constant
'winter' isotopic composition dominates
'summer' precipitation amount = +100%, 'winter precipitation amount= constant
'summer' precipitation amount = 0
'winter' precipitation amount= constant
DECADAL PRECIPITATION δ18O CHANGE
PRECIPITATION AMOUNT CHANGE FOR 'SUMMER' AND 'WINTER' (FRACTIONAL CHANGE)
1
0.5
0
-0.5
-1
-1.5
-1
-0.5
0
0.5
1

Figure 3

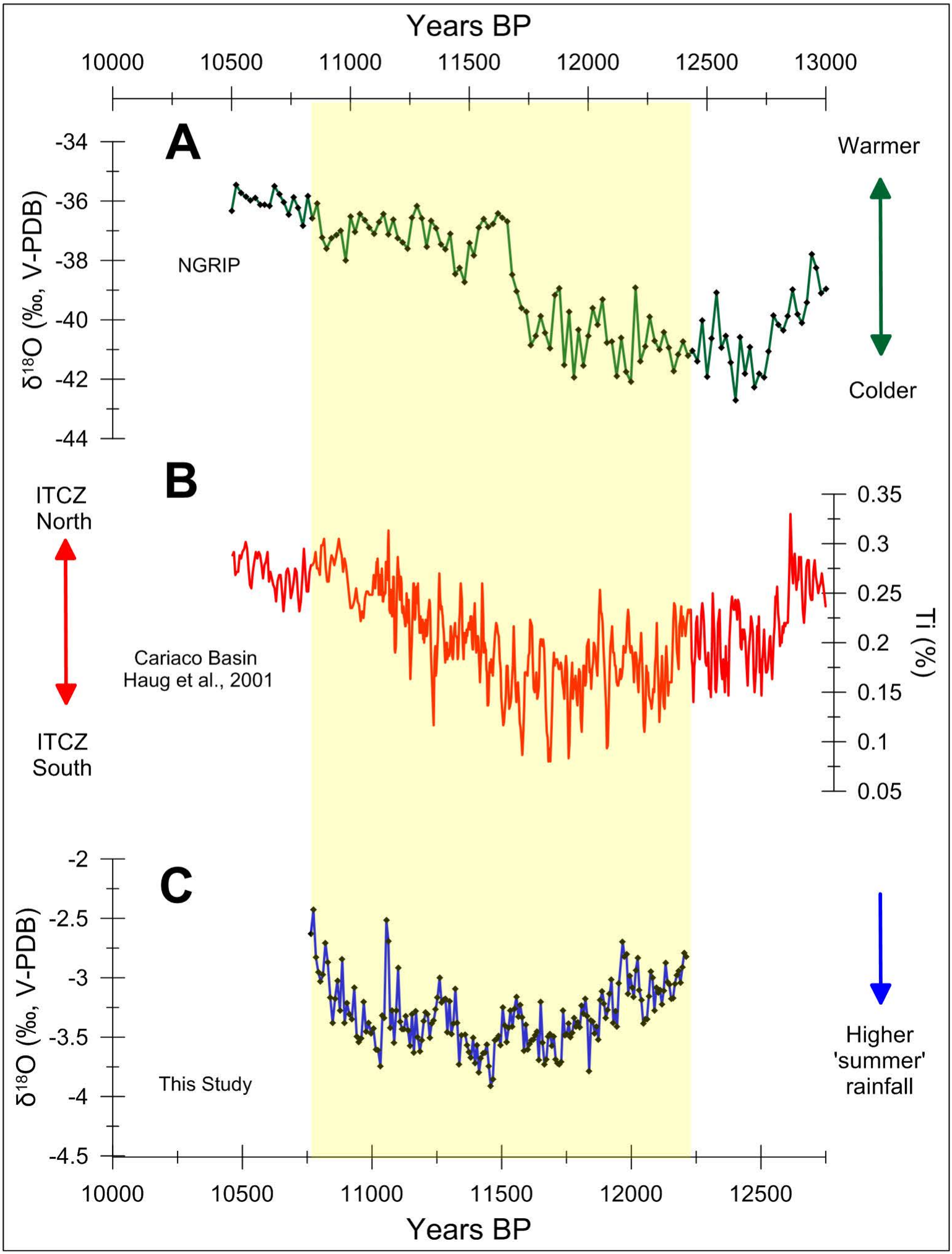
Years BP
10000
10500
11000
11500
12000
12500
13000
A
-34
-36
-38
-40
-42
-44
δ18O (‰, V-PDB)
NGRIP
Warmer
Colder
B
ITCZ
North
ITCZ
South
Cariaco Basin
Haug et al., 2001
0.35
0.3
0.25
0.2
0.15
0.1
0.05
Ti (%)
C
-2
-2.5
-3
-3.5
-4
-4.5
δ18O (‰, V-PDB)
This Study
Higher
'summer'
rainfall
10000
10500
11000
11500
12000
12500
Years BP

Figure 4

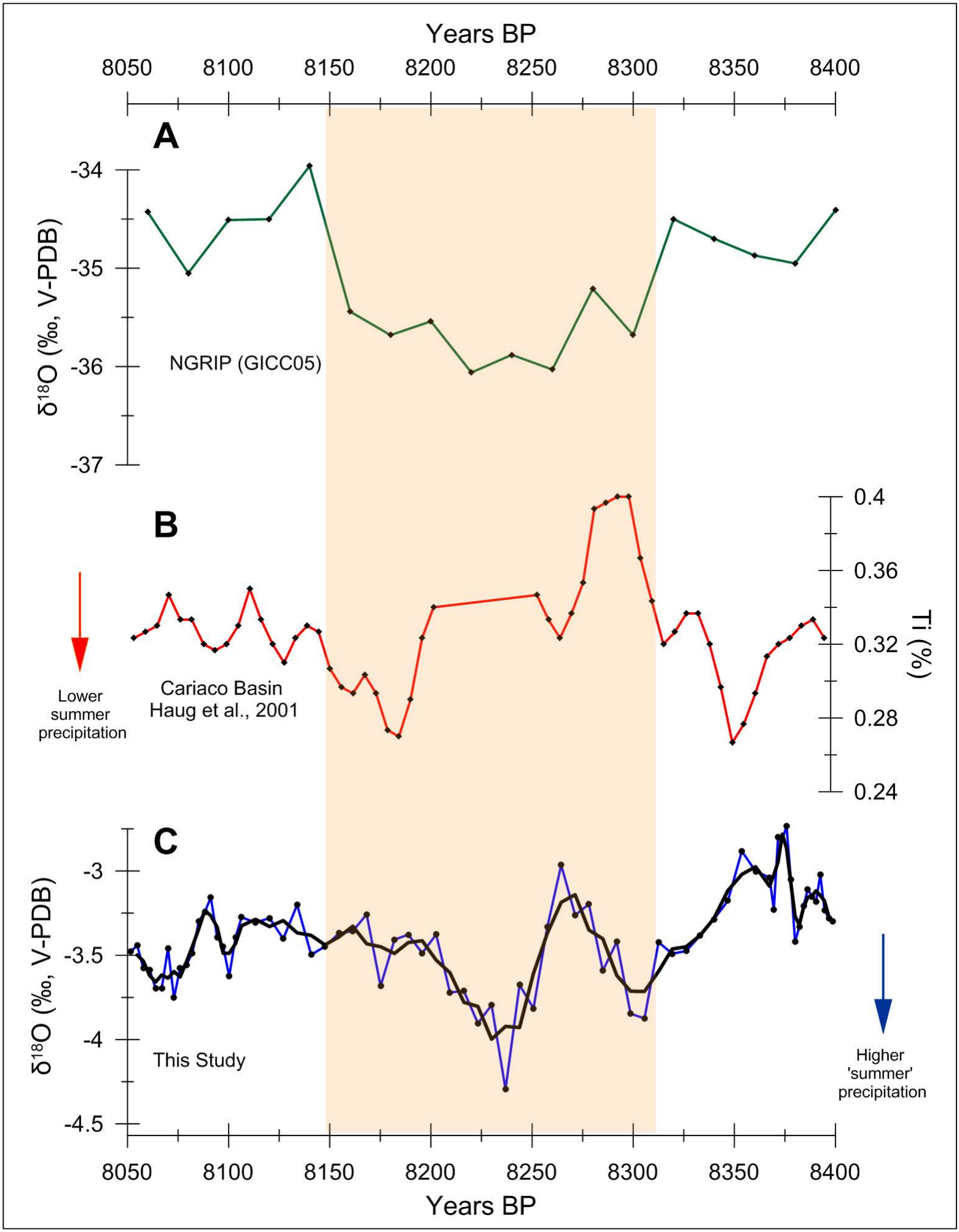
Years BP
8050
8100
8150
8200
8250
8300
8350
8400
A
-34
-35
-36
-37
δ18O (‰, V-PDB)
NGRIP (GICC05)
B
0.4
0.36
0.32
0.28
0.24
Ti (%)
Lower summer precipitation
Cariaco Basin
Haug et al., 2001
C
-3
-3.5
-4
-4.5
δ18O (‰, V-PDB)
This Study
Higher 'summer' precipitation
Years BP

Figure 5

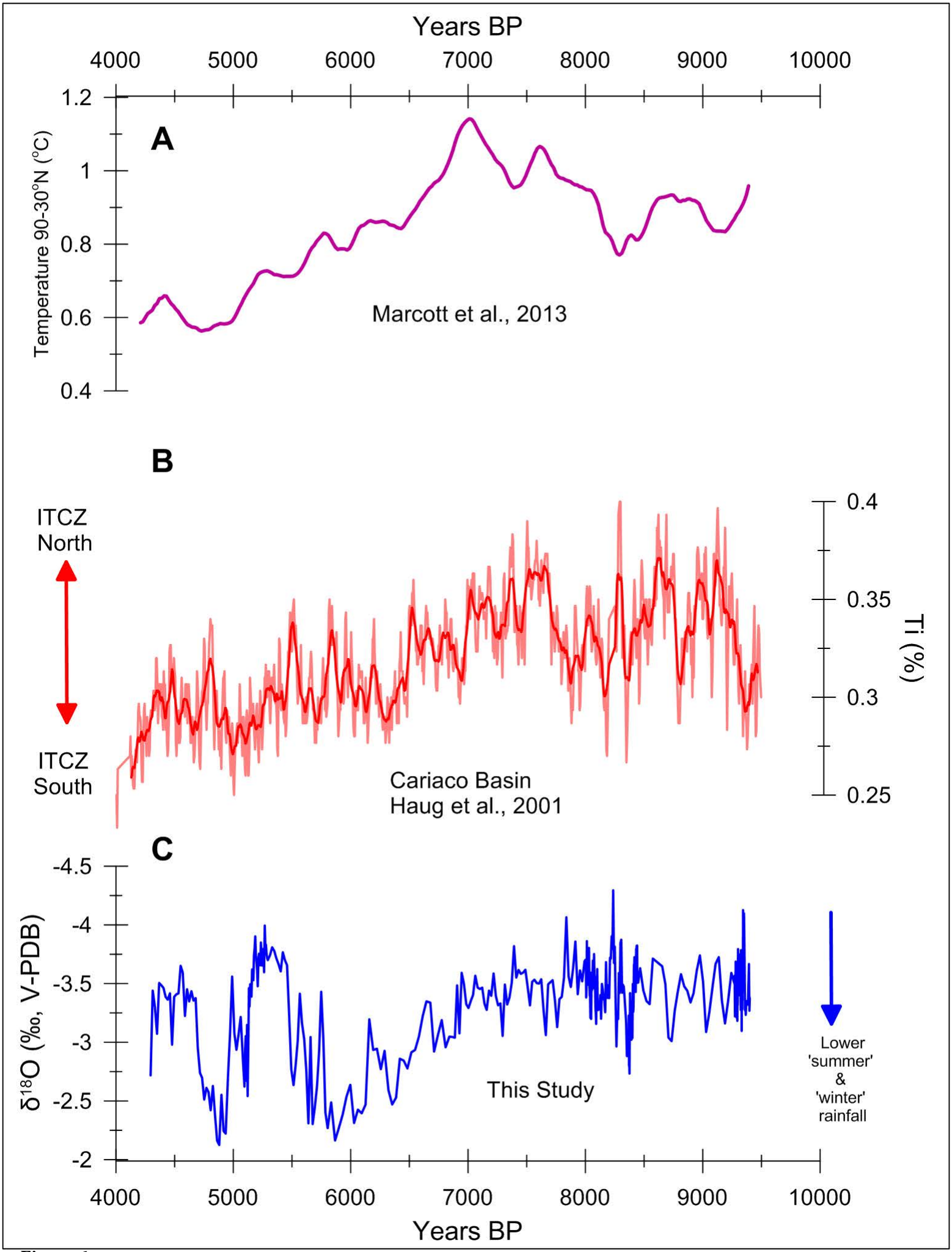
Years BP
4000
5000
6000
7000
8000
9000
10000
A
Temperature 90-30°N (°C)
1.2
1
0.8
0.6
0.4
Marcott et al., 2013
B
ITCZ
North
ITCZ
South
Cariaco Basin
Haug et al., 2001
0.4
0.35
0.3
0.25
Ti (%)
C
δ18O (‰, V-PDB)
-4.5
-4
-3.5
-3
-2.5
-2
This Study
Lower
'summer'
&
'winter'
rainfall
Years BP

Figure 6

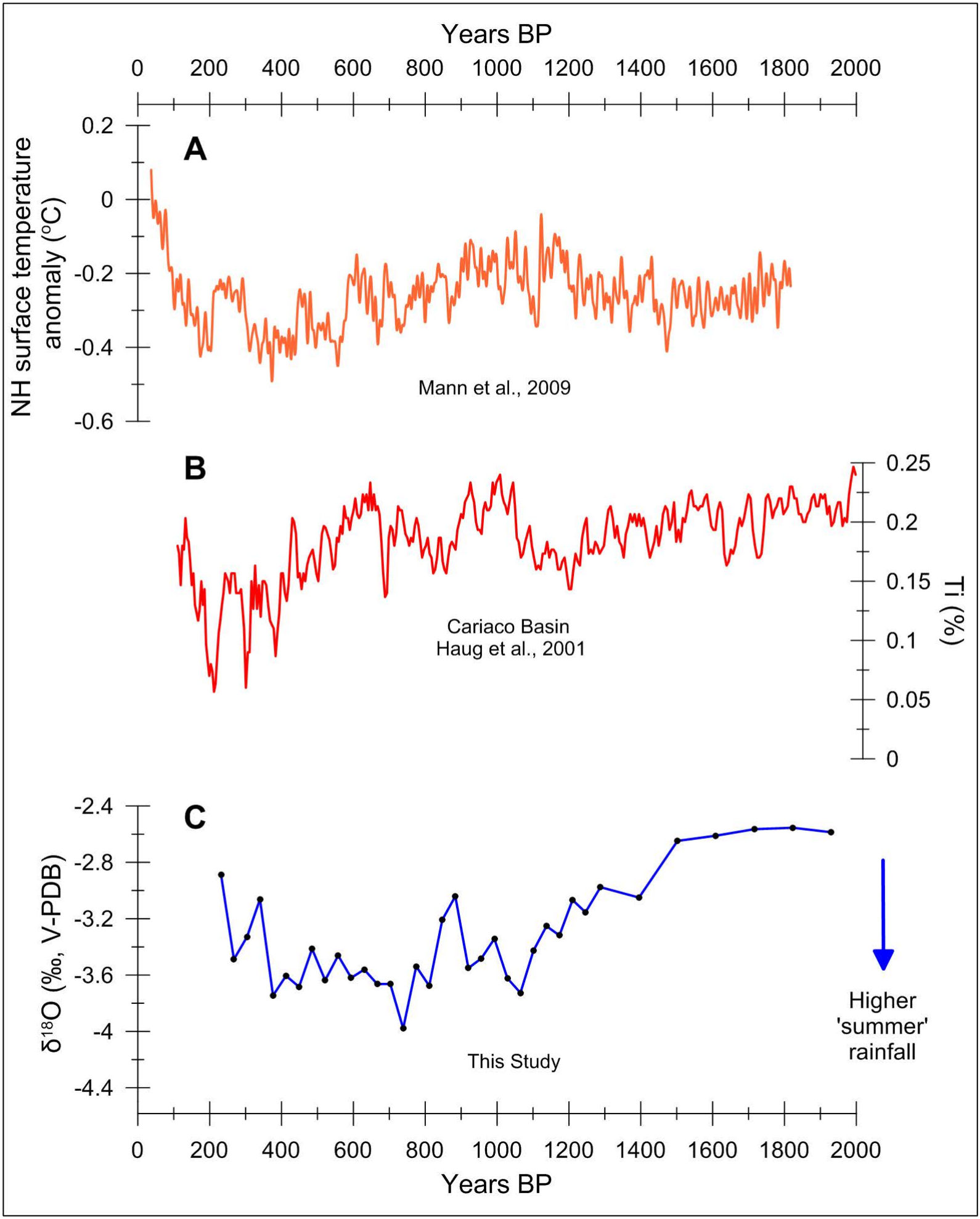
Years BP
0
200
400
600
800
1000
1200
1400
1600
1800
2000
A
NH surface temperature anomaly (°C)
0.2
0
-0.2
-0.4
-0.6
Mann et al., 2009
B
0.25
0.2
0.15
0.1
0.05
0
Ti (%)
Cariaco Basin
Haug et al., 2001
C
-2.4
-2.8
-3.2
-3.6
-4
-4.4
δ18O (‰, V-PDB)
This Study
Higher 'summer' rainfall
Years BP

Figure 7